

NONLINEAR STABILITY OF THE IMPLICIT-EXPLICIT METHODS FOR THE ALLEN-CAHN EQUATION

XINLONG FENG^{1,2}, HUAILING SONG^{2,3}
TAO TANG^{2*} AND JIANG YANG²

¹ College of Mathematics and System Sciences
Xinjiang University
Urumqi 830046, China

² Institute of Theoretical and Computational Studies
& Department of Mathematics
Hong Kong Baptist University
Kowloon Tong, Hong Kong, China

³ School of Mathematics
Hunan University
Changsha, Hunan, China

ABSTRACT. In this paper, we will investigate the first- and second-order implicit-explicit schemes with parameters for solving the Allen-Cahn equation. It is known that the Allen-Cahn equation satisfies a nonlinear stability property, i.e., the free-energy functional decreases in time. The goal of this paper is to consider implicit-explicit schemes that inherit the nonlinear stability of the continuous model, which will be achieved by properly choosing parameters associated with the implicit-explicit schemes. Theoretical justifications for the nonlinear stability of the schemes will be provided, and the theoretical results will be verified by several numerical examples.

1. Introduction. This paper is concerned with numerical approximations of the Allen-Cahn equation

$$(1) \quad \frac{\partial u}{\partial t} = \epsilon \Delta u - f(u), \quad (x, t) \in \Omega \times (0, T],$$

with the initial condition

$$(2) \quad u|_{t=0} = u_0,$$

and the homogeneous Dirichlet boundary condition

$$(3) \quad u|_{\partial\Omega} = 0.$$

It is pointed out that Problem (1)-(2) can be also equipped with the periodic boundary condition, or the Neumann boundary condition $\frac{\partial u}{\partial n}|_{\partial\Omega} = 0$, where n denotes the unit outward normal vector on Ω . In the latter case we also need to impose a mass conservation.

In problem (1)-(3), u represents the concentration of one of the two metallic components of the alloy, the positive parameter ϵ represents the inter-facial width which is small compared to the characteristic length of the laboratory scale, $\Omega \subset \mathcal{R}^d$ ($d = 1, 2, 3$) is a bounded domain, $f(u) = F'(u)$ with $F(u)$ being a given

2010 *Mathematics Subject Classification.* 65M06, 65M12, 6506, 35k20, 35Q56.

Key words and phrases. Implicit-explicit scheme, Allen-Cahn equation, energy stability.

* Corresponding author.

energy potential. The Allen-Cahn equation was originally introduced by Allen and Cahn in [1] to describe the motion of anti-phase boundaries in crystalline solids. The homogeneous boundary conditions imply that none of the mixtures can pass through the boundary walls. The Allen-Cahn equation has been widely used to model various phenomena in nature. In particular, it has become a basic model equation for the diffuse interface approach developed to study phase transitions and interfacial dynamics in materials science [10, 13, 18].

An important feature of the Allen-Cahn equation is that the problem can be characterized by the Liapunov energy functional

$$(4) \quad E(u) = \int_{\Omega} \left(\frac{\epsilon}{2} |\nabla u|^2 + F(u) \right) dx$$

in L^2 . By taking the inner product for Eq. (1) with $-\epsilon\Delta u + f(u)$, we can obtain the energy law for problem (1)-(3):

$$(5) \quad \frac{\partial E(u(t))}{\partial t} = - \int_{\Omega} |-\epsilon\Delta u + f(u)|^2 dx,$$

which yields the following energy-decay property:

$$(6) \quad E(u(t_n)) \leq E(u(t_m)), \quad \forall t_n > t_m.$$

Designing numerical schemes for phase field models that satisfy the energy property of the form (6) has been extensively studied in the past. With the time discretization, we particularly mention the work of Eyre [11] who derived a first-order accurate nonlinearly energy stable time-stepping scheme for phase field models. Although Eyre's work is unpublished, it has had significant impact in the phase field simulation community. In particular, it has served as inspiration for many other time integration schemes in recent years, see, e.g., [12, 9, 8, 27, 28].

It is observed that the Allen-Cahn equation involves a small positive parameter in the diffusion term, which normally leads to a stiff system after spatial discretizations. In this case, the Implicit-Explicit (IMEX) technique, which has been introduced for time dependent partial differential equations, usually can play an important role, see, e.g., [2, 3]. The IMEX schemes use an implicit scheme for the diffusion term and an explicit scheme for the convection term. Some schemes of this type were proposed and analyzed as far back as the late 1970's; we refer to [7, 14, 16] for recent developments.

In this work, we will consider IMEX approximations for the Allen-Cahn equation (1). Our goal is to obtain stable first- and second-order time-accurate schemes. The key idea is to find the feasible range of parameters involving in the IMEX schemes so that the nonlinear stability property like (6) is satisfied.

The rest of the paper is organized as follows. In Section 2, we introduce the general linear multistep implicit-explicit schemes with parameters. In Section 3, we show that a number of time discretization schemes satisfying the energy decaying property. In Section 4, several numerical experiments are carried out, where fourth-order compact difference schemes are employed in spatial discretization. The nonlinear stability is observed in the numerical experiments. Concluding remarks and possible extensions will be presented in the final section.

2. General linear multistep implicit-explicit schemes. Assume that all the spatial derivatives in the Allen-Cahn equation (1) have been discretized by certain difference methods. This gives rise to a large system of ordinary differential

equations in time which typically has the form

$$(7) \quad \frac{dU}{dt} = \epsilon AU + B(U),$$

where A is a constant matrix and B is a nonlinear operator for U . We now introduce k -step implicit-explicit schemes for Eq. (7). Letting τ be the time-step and U^n denote the approximate solution at $t_n = n\tau$, we may obtain from (7) that

$$(8) \quad \frac{1}{\tau} \left(U^{n+1} + \sum_{j=0}^{k-1} \alpha_j U^{n-j} \right) = \epsilon \sum_{j=-1}^{k-1} \beta_j AU^{n-j} + \sum_{j=0}^{k-1} \gamma_j B(U^{n-j}),$$

where $\beta_{-1} \neq 0$. Assume that function $U(t)$ is smooth enough. Using Taylor expansion at $t_n = n\tau$ gives the following truncation error

$$(9) \quad \begin{aligned} & \frac{1}{\tau} \left(1 + \sum_{j=0}^{k-1} \alpha_j \right) U(t_n) + \left(1 - \sum_{j=1}^{k-1} j\alpha_j \right) U^{(1)}(t_n) + \dots \\ & + \frac{\tau^{p-1}}{p!} \left(1 + \sum_{j=1}^{k-1} (-j)^p \alpha_j \right) U^{(p)}(t_n) \\ & - \epsilon \sum_{j=-1}^{k-1} \beta_j AU(t_n) - \tau \epsilon \left(\beta_{-1} - \sum_{j=-1}^{s-1} \beta_j \right) A\dot{U}(t_n) - \dots \\ & - \frac{\tau^{p-1}}{(p-1)!} \epsilon \left(\beta_{-1} + \sum_{j=0}^{k-1} \beta_j (-j)^{p-1} \right) AU^{(p-1)}(t_n) - \sum_{j=0}^{k-1} \gamma_j B(U(t_n)) \\ & + \tau \sum_{j=1}^{k-1} j\gamma_j B^{(1)} - \dots - \frac{\tau^{p-1}}{(p-1)!} \sum_{j=1}^{k-1} (-j)^{p-1} \gamma_j B^{(p-1)} = o(\tau^p), \end{aligned}$$

where $U^{(i)}(t_n)$ denotes the i th-order derivative of function U at t_n , and $B^{(i)}$ denotes the i th-order derivative of function B at $u(t_n)$, $i \geq 1$. Applying the original equation to the truncation error, we obtain p th-order scheme provided the following conditions hold:

$$(10) \quad \begin{aligned} & 1 + \sum_{j=0}^{k-1} \alpha_j = 0, \\ & 1 - \sum_{j=1}^{k-1} j\alpha_j = \sum_{j=-1}^{k-1} \beta_j = \sum_{j=0}^{k-1} \gamma_j, \\ & \vdots \\ & \frac{1}{p!} \left(1 + \sum_{j=1}^{k-1} (-j)^p \alpha_j \right) = \frac{1}{(p-1)!} \left(\beta_{-1} + \sum_{j=1}^{k-1} \beta_j (-j)^{p-1} \right) = \frac{1}{(p-1)!} \sum_{j=1}^{k-1} (-j)^{p-1}. \end{aligned}$$

It follows from [2, 3] that the family of k -step implicit-explicit schemes of order k has k parameters, and the k -step implicit-explicit scheme can not have order of accuracy greater than k . Below we will present the first- and second-order implicit-explicit schemes with parameters by solving the underdetermined system (10).

2.1. First-order implicit-explicit schemes. The first-order implicit-explicit schemes for ODEs can be written as

$$(11) \quad \frac{U^{n+1} - U^n}{\tau} = \epsilon A[\alpha U^{n+1} + (1 - \alpha)U^n] + B(U^n)$$

where α is a free parameter. Here we restrict $\alpha > 0$ to prevent large truncation error and ensure the schemes having good stability.

We point out that choosing $\alpha = 1$ the backward Euler scheme. If $\alpha = \frac{1}{2}$ and $B(U^n)$ is replaced by $(B(U^n) + B(U^{n+1}))/2$, then we obtain the second-order nonlinear Crank-Nicolson scheme.

2.2. Second-order implicit-explicit schemes. If we center our schemes in time about time step $t_{n-\alpha/(4+2\alpha)}$, the second-order implicit-explicit schemes can be written as

$$(12) \quad \begin{aligned} & \frac{U^{n+1} + \alpha U^n - (1 + \alpha)U^{n-1}}{\tau} \\ &= \epsilon A \left(\left(\beta - \frac{\alpha}{2} \right) U^{n+1} + \left(2 + \frac{3}{2}\alpha - 2\beta \right) U^n + \beta U^{n-1} \right) \\ & \quad + \left(\left(2 + \frac{\alpha}{2} \right) B(U^n) + \frac{\alpha}{2} B(U^{n-1}) \right), \end{aligned}$$

where α and β are two free parameters. Here we restrict $\beta \geq \frac{\alpha}{2}$ to prevent large truncation error and ensure better stability. Some special cases are classical, e.g,

- If $(\alpha, \beta) = (-1, 0)$, then we have the Crank-Nicolson/Adams-Bashforth scheme.

$$(13) \quad \frac{U^{n+1} - U^n}{\tau} = \epsilon A \frac{U^{n+1} + U^n}{2} + \left(\frac{3}{2} B(U^n) - \frac{1}{2} B(U^{n-1}) \right).$$

- If $(\alpha, \beta) = (-1, \frac{1}{16})$, then we obtain the modified Crank-Nicolson/Adams-Bashforth scheme

$$(14) \quad \begin{aligned} & \frac{U^{n+1} - U^n}{\tau} \\ &= \epsilon A \left(\frac{9}{16} U^{n+1} + \frac{3}{8} U^n + \frac{1}{16} U^{n-1} \right) + \left(\frac{3}{2} B(U^n) - \frac{1}{2} B(U^{n-1}) \right). \end{aligned}$$

- If $(\alpha, \beta) = (-\frac{4}{3}, 0)$, then we have semi-implicit backward difference formula (BDF)

$$(15) \quad \frac{3U^{n+1} - 4U^n + U^{n-1}}{2\tau} = \epsilon A U^{n+1} + (2B(U^n) - B(U^{n-1})).$$

- If $(\alpha, \beta) = (0, 1)$, we have semi-implicit Leap-Frog formula

$$(16) \quad \frac{U^{n+1} - U^{n-1}}{2\tau} = \epsilon A \frac{U^{n+1} + U^{n-1}}{2} + B(U^n)$$

We point out that there is a close relationship between the first- and second-order schemes described above and the stabilized schemes proposed in [15, 25, 26, 27]. In the latter cases, suitable $O(\tau U_t)$ or $(\tau^2 U_{tt})$ terms are added in order to stabilize the time discretizations. To see this, let us rewrite the first term on the right-hand side of (11) as

$$\epsilon A[\alpha U^{n+1} + (1 - \alpha)U^n] = \epsilon A U^{n+1} + (\alpha - 1)\epsilon A(U^{n+1} - U^n),$$

and the first term on right-hand side of (12) as

$$\begin{aligned} & \epsilon A[(\beta - \frac{\alpha}{2})U^{n+1} + (2 + \frac{3}{2}\alpha - 2\beta)U^n + \beta U^{n-1}] \\ &= \epsilon A[-\frac{\alpha}{2}U^{n+1} + (2 + \frac{3}{2}\alpha)U^n] + \beta \epsilon A(U^{n+1} - 2U^n + U^{n-1}). \end{aligned}$$

We can obtain relevant stabilized first-order and second-order schemes as given in [15, 27, 26, 25] by choosing suitable parameters. More precisely, this can be done by adding $(\alpha - 1)\tau\epsilon AU_t$ in the first-order scheme and $\beta\tau^2\epsilon AU_{tt}$ in the second-order scheme.

3. Stability of the IMEX schemes. We first introduce some notations which will be used in the remaining of the paper. We use $H^m(\Omega)$ and $\|\cdot\|_m (m = 0, \pm 1, \dots)$ to denote the standard Sobolev spaces and their norms, respectively. In particular, the norm and inner product of $L^2(\Omega) = H^0(\Omega)$ are denoted by $\|\cdot\|_0$ and (\cdot, \cdot) respectively. Without loss of generality, we restrict our attention to potential function $F(u)$ whose derivative $f(u) = F'(u)$ satisfies the following condition: there exists a positive constant L such that the $f'(u)$ is bounded, i.e.,

$$(17) \quad |f'(u)| \leq L, \quad \forall u \in \mathcal{R}.$$

This condition has been used in a number of previous papers, see, e.g., [25]. As this assumption is crucial in the analysis of this work, we will reiterate the reasoning behind this assumption here. Very often the following Ginzburg-Landau double-well potential has been widely used:

$$F(u) = \frac{1}{4}(u^2 - 1)^2.$$

However, its quartic growth at infinity introduces various technical difficulties in the analysis and approximation of Allen-Cahn equations. Since it is well-known that the Allen-Cahn equation satisfies the maximum principle, we can truncate $F(u)$ to quadratic growth outside of the interval $[-M, M]$ without affecting the solution if the maximum norm of the initial condition u_0 is bounded by M . A typical truncated double-well potential is constructed in [25], where it is shown that there exists an L such that (17) is satisfied with the truncated double-well potential.

3.1. First-order IMEX schemes. Taking inner product with $V \in H_0^1(\Omega)$, we have the first-order implicit-explicit method

$$(18) \quad \frac{(U^{n+1} - U^n, V)}{\tau} + \epsilon(\nabla(\alpha U^{n+1} + (1-\alpha)U^n), \nabla V) + (f(U^n), V) = 0, \quad \forall V \in H_0^1(\Omega).$$

Under reasonable assumptions, we prove that the above scheme is energy stable in the sense of (6).

Theorem 3.1. *Consider the scheme (18) with the boundary condition (3). If*

$$(19) \quad \alpha \geq \frac{1}{2}, \quad \tau \leq \frac{2}{L},$$

where L is defined by (17), then the energy-decay property (6) holds, i.e.,

$$(20) \quad E(U^{n+1}) \leq E(U^n), \quad \forall n \geq 0.$$

Proof. Taking $V = U^{n+1} - U^n$ in (18) and using the identity

$$(\phi - \varphi, 2\phi) = \|\phi\|^2 - \|\varphi\|^2 + \|\phi - \varphi\|^2,$$

yield

$$(21) \quad \begin{aligned} & \frac{1}{\tau} \|U^{n+1} - U^n\|_0^2 + \left(\alpha - \frac{1}{2}\right) \epsilon \|\nabla(U^{n+1} - U^n)\|_0^2 \\ & + \frac{\epsilon}{2} (\|\nabla U^{n+1}\|_0^2 - \|\nabla U^n\|_0^2) + (f(U^n), U^{n+1} - U^n) = 0. \end{aligned}$$

The above result, together with the Taylor formula

$$(22) \quad F(U^{n+1}) - F(U^n) = f(U^n)(U^{n+1} - U^n) + \int_{U^n}^{U^{n+1}} f'(s)(U^{n+1} - s) ds$$

and the definition (4), give

$$(23) \quad \begin{aligned} & E(U^{n+1}) - E(U^n) + \left(\alpha - \frac{1}{2}\right) \epsilon \|\nabla(U^{n+1} - U^n)\|_0^2 + \frac{1}{\tau} \|U^{n+1} - U^n\|_0^2 \\ & = \int_{\Omega} \int_{U^n}^{U^{n+1}} f'(s)(U^{n+1} - s) ds dx. \end{aligned}$$

This, together with the mean-value theorem and (17), gives

$$(24) \quad \begin{aligned} & E(U^{n+1}) - E(U^n) + \left(\alpha - \frac{1}{2}\right) \epsilon \|\nabla(U^{n+1} - U^n)\|_0^2 + \frac{1}{\tau} \|U^{n+1} - U^n\|_0^2 \\ & = \frac{1}{2} (f'(\xi^n)(U^{n+1} - U^n), U^{n+1} - U^n) \\ & \leq L \int_{\Omega} \int_{U^n}^{U^{n+1}} (U^{n+1} - s) ds dx = \frac{L}{2} \|U^{n+1} - U^n\|_0^2. \end{aligned}$$

The desired result follows from (24) and the assumption (19). \square

It is obvious that as the positive parameter α increases the scheme has better stability. On the other hand, from (18) we obtain the first term of truncation error as follows

$$\left(\frac{1}{2} U^{(2)}(t_n) - \alpha \epsilon A U^{(1)}(t_n) \right) \tau.$$

This implies that larger values of α may lead to larger truncation errors.

Furthermore, if we use the Dirichlet-Poincaré inequality

$$\int_a^b |u(x)|^2 dx \leq (b-a)^2 \int_a^b |u'(x)|^2 dx,$$

we can obtain from the proof of the above theorem that

$$E(U^{n+1}) - E(U^n) + \left(\frac{(\alpha - \frac{1}{2})\epsilon}{(b-a)^2} + \frac{1}{\tau} - \frac{L}{2} \right) \|U^{n+1} - U^n\|_0^2 \leq 0.$$

Consequently, if (19) is satisfied, then the energy-decay holds provided that

$$(25) \quad \alpha \geq \frac{1}{2} + \left(\frac{L}{2} - \frac{1}{\tau} \right) \frac{(b-a)^2}{\epsilon}.$$

3.2. Second-order IMEX schemes. Taking inner product with $V \in H_0^1(\Omega)$ or $H^1(\Omega)$, we have the second-order implicit-explicit method

$$\begin{aligned}
 & \frac{(U^{n+1} + \alpha U^n - (1 + \alpha)U^{n-1}, V)}{\tau} \\
 & + \epsilon \left(\nabla \left((\beta - \frac{\alpha}{2})U^{n+1} + (2 + \frac{3}{2}\alpha - 2\beta)U^n + \beta U^{n-1} \right), \nabla V \right) \\
 (26) \quad & + \left((2 + \frac{\alpha}{2})f(U^n) + \frac{\alpha}{2}f(U^{n-1}), V \right) = 0.
 \end{aligned}$$

Under reasonable assumptions, we show that the second-order implicit-explicit schemes are energy stable.

Theorem 3.2. *In the second-order implicit-explicit scheme (26), if $\tau \leq (2 + \alpha)/L$ and either of*

$$(27) \quad \beta \geq 0, \quad -2 < \alpha \leq -1$$

or

$$(28) \quad -\frac{1}{2} < \beta \leq 0, \quad -2 < \alpha \leq 2\beta - 1$$

is satisfied, then (26) is energy-stable in the following sense:

$$\begin{aligned}
 & E(U^{n+1}) + \eta_1 \|\nabla(U^{n+1} - U^n)\|_0^2 + \eta_2 \|U^{n+1} - U^n\|_0^2 \\
 (29) \quad & \leq E(U^n) + \eta_1 \|\nabla(U^n - U^{n-1})\|_0^2 + \eta_2 \|U^n - U^{n-1}\|_0^2,
 \end{aligned}$$

for all $n \geq 0$, where η_1, η_2 are two positive constants.

Proof. Taking $V = U^{n+1} - U^n$ in (26) and using the Taylor expansion similar to (22) twice yield:

$$\begin{aligned}
 (30) \quad & E(U^{n+1}) - E(U^n) + \frac{\|U^{n+1} - U^n\|_0^2 + (1 + \alpha)(U^{n+1} - U^n, U^n - U^{n-1})}{\tau(2 + \alpha)} \\
 & + \frac{(\beta - 1 - \alpha)\epsilon}{2 + \alpha} \|\nabla(U^{n+1} - U^n)\|^2 - \frac{\beta\epsilon}{2 + \alpha} (\nabla(U^{n+1} - U^n), \nabla(U^n - U^{n-1})) \\
 & = \left(\int_{U^n}^{U^{n+1}} f'(s)(U^{n+1} - s)ds, 1 \right) - \frac{\alpha}{2(2 + \alpha)} \left(\int_{U^{n-1}}^{U^n} f'(s)ds, U^{n+1} - U^n \right) \\
 & \leq \frac{L}{2} \|U^{n+1} - U^n\|_0^2 + \frac{|\alpha|L}{2|2 + \alpha|} \|U^{n+1} - U^n\|_0 \|U^n - U^{n-1}\|_0.
 \end{aligned}$$

Using Hölder’s inequality, we have the following inequality

$$\begin{aligned}
 & E(U^{n+1}) + C_1 \|\nabla(U^{n+1} - U^n)\|_0^2 + C_2 \|U^{n+1} - U^n\|_0^2 \\
 (31) \quad & \leq E(U^n) + C_3 \|\nabla(U^n - U^{n-1})\|_0^2 + C_4 \|U^n - U^{n-1}\|_0^2,
 \end{aligned}$$

where

$$\begin{aligned}
 C_1 &= \frac{(\beta - 1 - \alpha)\epsilon}{2 + \alpha} - \frac{|\beta|\epsilon}{2|2 + \alpha|}, & C_3 &= \frac{|\beta|\epsilon}{2|2 + \alpha|} \\
 C_2 &= \frac{1}{\tau(2 + \alpha)} - \frac{|1 + \alpha|}{2\tau|2 + \alpha|} - \frac{L}{2} - \frac{|\alpha|L}{4|2 + \alpha|}, & C_4 &= \frac{|\alpha|L}{4|2 + \alpha|} + \frac{|1 + \alpha|}{2\tau|2 + \alpha|}.
 \end{aligned}$$

To establish the energy-decay property, we first restrict the choice of parameters by requiring

$$0 \leq C_3 \leq C_1 \quad \text{and} \quad 0 \leq C_4 \leq C_2.$$

Clearly, $C_3 \geq 0$ and $C_4 \geq 0$. Moreover, it is natural to assume that $2 + \alpha > 0$. Simple computation shows that if

$$(32) \quad \alpha \in (-2, -1] \quad \text{and} \quad \beta \geq 0$$

or

$$(33) \quad \alpha \in (-2, 2\beta - 1] \quad \text{and} \quad \beta \in \left(-\frac{1}{2}, 0\right]$$

is satisfied, then we have $C_1 \geq C_3$. On the other hand, if $\tau \leq (2 + \alpha)/L$, then $C_2 \geq C_4$. Setting $(\eta_1, \eta_2) = (C_3, C_4)$ yields the desired result (29). \square

Remark. Note that the discretized energy definition used in Theorem 3.2 (i.e., (29)) is an $O(\Delta t)$ perturbation of the original definition used in Theorem 3.1. In fact, this seems common for higher order discretizations (see, e.g., [26]): when the order of accuracy is increased, the relevant discretized energy has to be modified with some consistent perturbations.

It follows from (26) that the leading term in the truncation errors is given by

$$\left(\frac{2 + \alpha}{6} U_{ttt}(t_n) + \left(\frac{\alpha}{4} - \beta \right) \epsilon A U_{tt}(t_n) - \frac{\alpha}{4} f_{tt} \right) \tau^2.$$

Note that if $(\alpha, \beta) = (-4/3, 0)$, we have the classical semi-implicit BDF as this scheme is obtained by using Taylor expansion at $t = t_{n+1}$. However, if $\alpha \in (-4/3, 2)$, then the resulting schemes are obtained by using Taylor expansion at a time after t_{n+1} . Moreover, it is obvious that $\beta > 0$ can enhance the energy stability. Hence, if $\alpha \in (-4/3, 2)$ and $\beta > 0$, better stability is expected. This will be confirmed in the numerical experiment section.

We close this section by pointing out the results in the above two theorems can be easily extended to the case with Neumann boundary condition or periodic condition.

4. Numerical experiments. In this section, we present some numerical experiments to illustrate the theoretical results obtained in the previous section.

4.1. The Allen-Cahn equation in 1D.

Example 4.1. We first consider

$$(34) \quad u_t = \epsilon u_{xx} + u - u^3, \quad x \in [-1, 1],$$

with the initial and boundary conditions

$$u(x, 0) = 0.53x + 0.47 \sin(-1.5\pi x), \quad u(-1, t) = -1, \quad u(1, t) = 1.$$

The above problem has stable equilibria at $u = \pm 1$ and an unstable equilibrium at $u = 0$. One of the interesting features of this equation is the phenomenon of metastability. Regions of the solution that are near ± 1 will be flat, and the interface between such areas can remain unchanged over a very long timescale before changing suddenly.

For spatial discretization, we use a fourth-order compact scheme to approximate (34) (see, e.g., [19, 20]):

$$\left(1 + \frac{h^2}{12} \delta_x^2 \right) \frac{\partial u_i}{\partial t} = \epsilon \delta_x^2 u_i + \left(1 + \frac{h^2}{12} \delta_x^2 \right) (u_i - u_i^3),$$

where δ_x^2 denotes the second-order central difference operator.

Mesh	$\tau = 0.1$	$\tau/2$	$\tau/4$	$\tau/8$	$\tau/16$
$\ \hat{u}_{h,\tau} - u_{h,\tau}\ $	3.0529e-3	1.5742e-3	7.9852e-4	4.0100e-4	1.9972e-5
Rate	/	0.95552	0.97921	0.99378	1.0056

TABLE 1. Example 4.1: numerical accuracy of first-order IMEX scheme with $(\alpha, \beta) = (1, 0)$. Also $\epsilon = 0.01$ and $T = 5$.

Mesh	$\tau = 0.1$	$\tau/2$	$\tau/4$	$\tau/8$	$\tau/16$
$\ \hat{u}_{h,\tau} - u_{h,\tau}\ $	1.2588e-4	3.5477e-5	9.3755e-6	2.4071e-6	6.0956e-7
Rate	/	1.8271	1.9199	1.9616	1.9814

TABLE 2. Example 4.1: Numerical accuracy of second-order IMEX scheme with $(\alpha, \beta) = (-1.5, 1)$. Also $\epsilon = 0.01$ and $T = 5$.

To verify the numerical accuracy, we take the numerical solution $\hat{u}_{h,\tau}$ obtained using the first-order and second-order implicit-explicit scheme with $h = 1/32$ and $\tau = 10^{-3}$ as the exact solution as compared with the corresponding coarse time-stepping approximation. The L^2 -norm error and convergence rate for the first-order IMEX scheme with $(\alpha, \beta) = (1, 0)$ are shown in Table 1, while those for the second-order IMEX scheme with $(\alpha, \beta) = (-1.5, 1)$ are shown in Table 2. It is observed that above schemes give predicted orders of accuracy in time.

Figure 1 shows the time evolution of the Allen-Cahn equation for different time steps. It is observed from Fig. 1(a) that the initial hump is metastable and disappears before $t = 40$ as $\tau = 0.1$. However, the initial hump is metastable and disappears near $t = 45$ if a larger time-step $\tau = 0.5$ is used. In both cases we choose $(\alpha, \beta) = (0.5, 1)$. This indicates that the initial hump delays as τ increases. In [17], Kassam and Trefethen use the exponential time-differencing fourth-order Runge-Kutta method for time-stepping. Their results suggest that the initial hump disappears near $t = 45$, which is comparable to our coarse time-step results with $\tau = 0.5$.

The energy evolution for Example 4.1 solved by our first-order scheme with different parameters are shown in Figs. 2 and 3. In Fig. 2, we fix the parameters α and β ($\alpha = 1$ or 2 and $\beta = 0$). It is observed that the accuracy is improved as τ decreases. In Fig. 3, we fix $\tau = 0.1$ and vary α , and it is observed that the accuracy is affected if large values of α are used.

The results using second-order implicit-explicit scheme with different parameters are shown in Fig. 4, where we fix $\beta = 0$ and $\tau = 0.5$ and change α . In this case, it follows from Theorem 3.2 if α is not within the interval $(-2, -1]$ the energy stability may not be guaranteed. To test this, we choose $\alpha = -0.99$ and -2.01 (both are out of the $(-2, -1]$) and in both cases the energy curves violate the energy-decay property.

It is observed in Figs. 2-4 that nonlinear energy stability is preserved if the parameters satisfy the conditions stated in Theorems 3.1 and 3.2.

4.2. The Allen-Cahn equation in 2D.

Example 4.2. Consider problem (1) with $f(u) = u - u^3$ and with the initial condition

$$u_0(x, y) = 0.05 \sin(x) \sin(y), \quad (x, y) \in [0, 2\pi] \times [0, 2\pi].$$

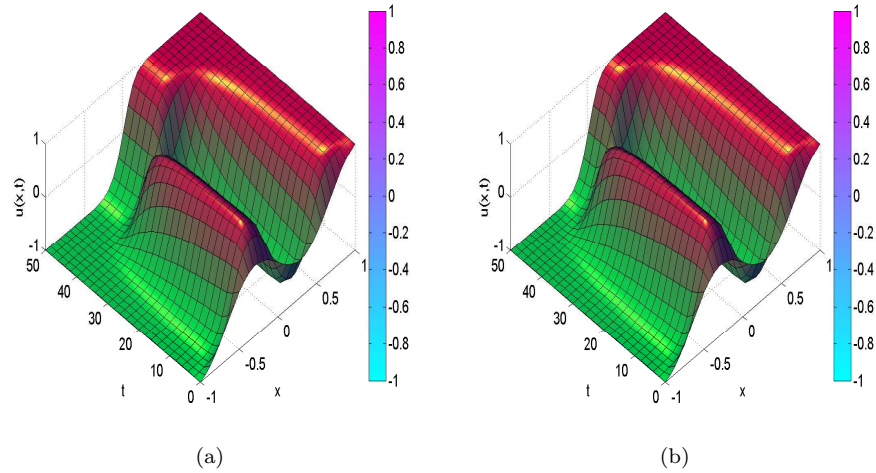


FIGURE 1. Time evolution for Example 4.1. (a). $\tau = 0.1$; in this case the initial hump is metastable and disappears before $t = 40$; (b). $\tau = 0.5$; in this case the initial hump disappears near $t = 45$.

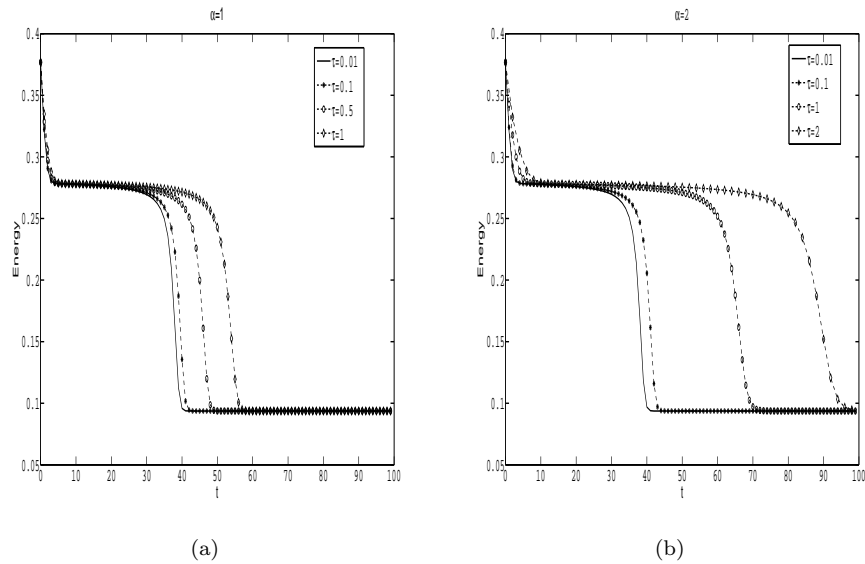
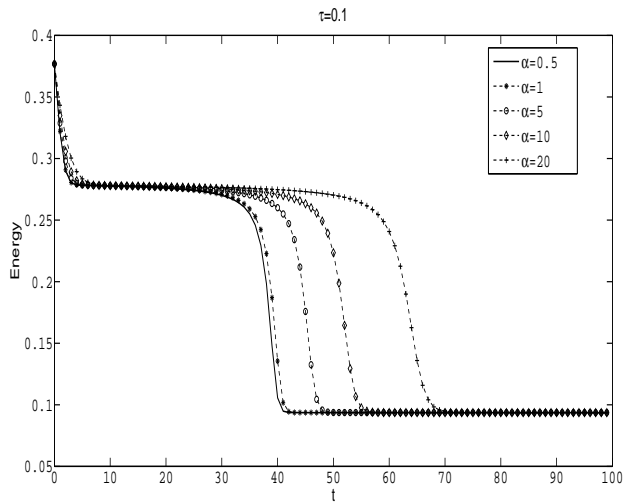


FIGURE 2. Example 4.1: the energy evolution using the first-order scheme. (a). Fix $\alpha = 1$ and take $\tau = 0.01, 0.1, 0.5, 1$. (b). Fix $\alpha = 2$ and change $\tau = 0.01, 0.1, 1, 2$.

The parameter ϵ will be chosen as 0.01. Firstly, the physical domain is partitioned with a $N \times N$ uniform grid. We using the following classical fourth-order compact



(a)

FIGURE 3. Example 4.1: the energy evolution with the first-order scheme. Fix $\tau = 0.1$ and take $\alpha = 0.5, 1, 5, 10, 20$. For any $\alpha \geq 0.5$, the method is stable, but the solution accuracy will become worse when α becomes larger.

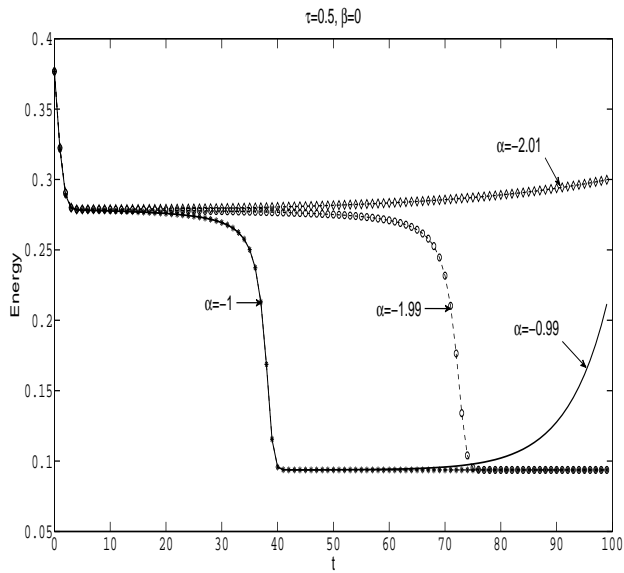


FIGURE 4. Example 4.1: the energy evolution using second-order scheme (12). The parameters $\tau = 0.5$ and $\beta = 0$ and $\alpha = -0.99, -1, -1.99, -2.01$.

scheme for the spatial discretization

$$(35) \quad \left(I + \frac{h^2}{12}(\delta_x^2 + \delta_y^2) \right) \frac{\partial u_i}{\partial t} = \epsilon \left(\delta_x^2 + \delta_y^2 + \frac{h^2}{6} \delta_x^2 \delta_y^2 \right) u_i + \left(I + \frac{h^2}{12}(\delta_x^2 + \delta_y^2) \right) (u_i - u_i^3).$$

To test the numerical accuracy, we take the numerical solution obtained using the second-order implicit-explicit scheme (12) with $N = 60$ and $\tau = 10^{-3}$ as the exact solution. The L^2 -norm error for $(\alpha, \beta) = (-1/5, 1)$ and $T = 1.2$ is shown in Table 4.2, from which it is clearly observed that above scheme gives desired (second) order of accuracy in time.

On the other hand, we consider the spatial discretization error as $(\alpha, \beta) = (1.9, 0)$. We take the numerical solution obtained using the second-order implicit-explicit scheme (12) with $N = 80$ and $\tau = 0.01$ as the exact solution. The convergence history at $T = 2$ is listed in Table 3, which shows that the rate of convergence is 4 in space.

Mesh	$\tau = 0.08$	$\tau/2$	$\tau/4$	$\tau/8$	$\tau/16$
$\ \hat{u}_{h,\tau} - u_{h,\tau}\ $	1.6795e-2	4.7255e-3	1.2497e-3	3.1904e-4	7.8431e-5
Rate	/	1.8295	1.9189	1.9697	2.0242

TABLE 3. Example 4.2: rate of convergence in time for scheme (12) for the 2D Allen-Cahn equation.

Mesh	$N = 10$	20	30	40	50
$\ \hat{u}_{h,\tau} - u_{h,\tau}\ $	4.1514e-1	2.7263e-2	5.2285e-3	1.5751e-3	5.8198e-4
Rate	/	4.1233	4.0729	4.1706	4.4618

TABLE 4. Example 4.2: rate of convergence in space for scheme (12) and (35) for the 2D Allen-Cahn equation.

We now study the effect of parameters for energy stability. Firstly, we choose $(\alpha, \beta, \tau) = (-4/3, 0, 0.01)$, i.e., the classical BDF method, to obtain the ‘accurate’ energy curve in Fig. 5(a). We then fix $\tau = 0.1$ and $\beta = 0$ and change α . It is observed in Fig. 5(b) if the values of α are chosen out of the $(-2, -1]$ (as given in Theorem 3.2), then the energy curves blow up within a finite time.

Furthermore, Fig. 5(b) shows the energy curves for $\tau = 0.2, \alpha = -4/3$ and variable β . In this case, $(\alpha, \beta) = (-3/4, 1)$ and $(-3/4, -0.5)$ do not satisfy the conditions (27) or (28) and the corresponding energy curves also blow up. For the case of $\beta = 0$, the condition (27) is satisfied and the corresponding energy decays are obtained.

Example 4.3. This example is the same as the last one, except that the initial condition is a random state by randomly distributing numbers from -0.01 to 0.01 to each grid point.

We take the parameter $\epsilon=0.01$ and $\tau = 0.1$, and the domain is $\Omega = [0, 2\pi] \times [0, 2\pi]$. The physical domain is partitioned with a 80×80 uniform grid. For this example, it is also observed that if the parameters α and β satisfy (27) or (28) then energy stability is preserved. To show an example, we use the second-order implicit-explicit scheme (12) together with the fourth order compact scheme (35) with $\alpha = -3/2$ and $\beta = 1$. As then given α and β satisfy (27) it is expected that the energy will be

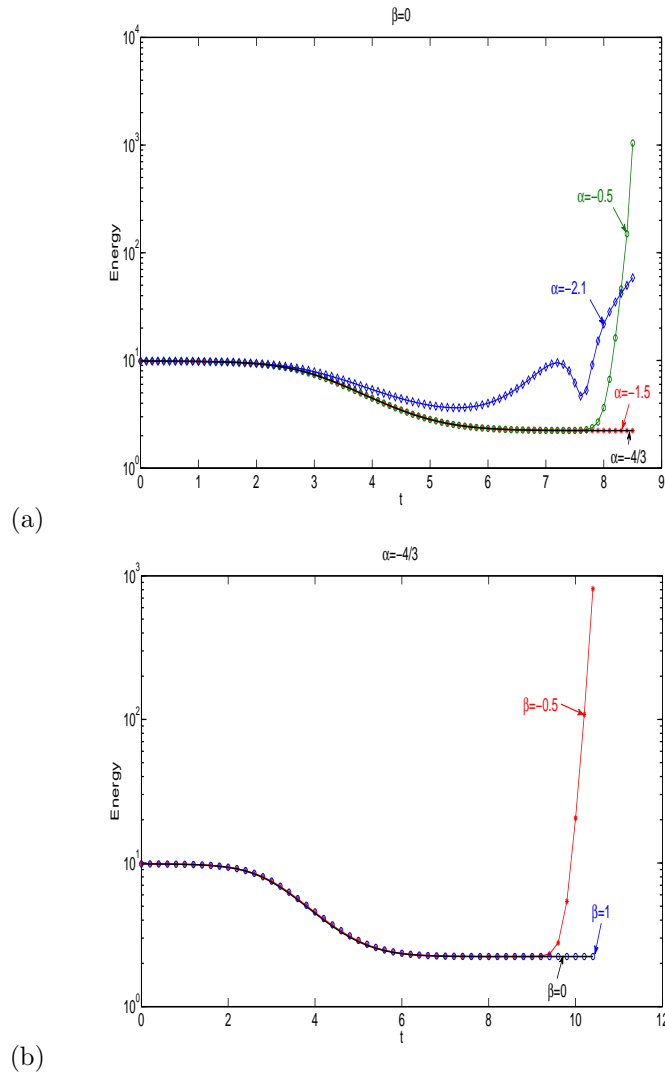


FIGURE 5. Example 4.2: the energy evolution with second-order scheme (12) as (a): $\beta = 0, \tau = 0.1$, and $\alpha = -0.5, -3/4, -1.5, -2.1$, and (b): $\alpha = -3/4, \tau = 0.2$ and $\beta = -0.5, 0, 1$. The results show that if conditions (27)-(28) are satisfied then the energy stability is preserved; otherwise energy blow up maybe observed.

decreasing, which is observed in Fig. 6. The corresponding solution contours are plotted in 7.

5. **Conclusions.** In this paper, the implicit-explicit schemes with parameters are investigated for solving the Allen-Cahn equation. It is shown that the implicit-explicit schemes with suitably chosen parameters are energy stable. Two theorems are obtained which characterize the parameter ranges for both the first- and

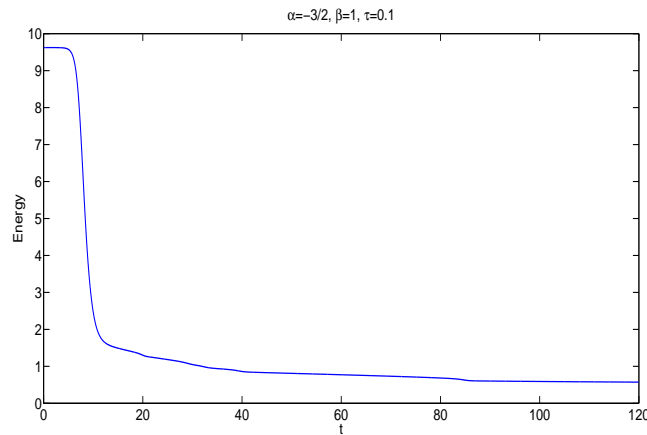


FIGURE 6. Example 4.3: the energy evolution for 2D Allen-Cahn equation with random initial distribution.

second-order time discretization. Numerical experiments are carried out to verify the theoretical predictions.

We first point out that although the method and the corresponding theory are developed in this work only for the Allen-Cahn equation it seems possible to extend them to other phase-field models.

The typical governing equations for the phase field models involve a small positive parameter, strong nonlinearity and higher-order derivatives in space. These difficulties require careful study of the numerical discretization methods. Another feature of the phase field computations is the large computational time involved, which makes the standard small constant time-stepping approach difficult due to rounding errors and computational resource constraints. If *both* the solution dynamics and the steady-state solutions are required, it is desirable to use some time-adaptivity strategy which allows to use small time steps in a few critical time levels (where the solution energy and solution change rapidly) and larger time steps in other time levels (where solution varies quite slowly). The highly stable time-stepping method obtained in this paper can be combined with some existing time-adaptivity strategies, see, e.g., [23, 29]

We close this paper by pointing out that there is a close relationship between phase-field equation (like Allen-Cahn and Cahn-Hilliard equations) and image processing, see, e.g., recent papers of Betozzi et al. [4, 5]. In particular, [6] outlines the use of a model for binary inpainting based on the Cahn-Hilliard equation, which allows for efficient inpainting of degraded text, as well as superresolution of high contrast images. Their models are simulated by using the (first-order) time-stepping technique known as convexity splitting given by Eyre [11]. It is certainly of interests to study high-order time discretization methods for solving image-related PDEs.

Acknowledgments. The first author is partially supported by the NSF of China (No.11271313) and Hong Kong Scholars Program. The second author is partially supported by Hunan University and Hong Kong Baptist University's Institute of Computational and Theoretical Studies. This research is partially supported by Hong Kong Research Grant Council and Hong Kong Baptist University.

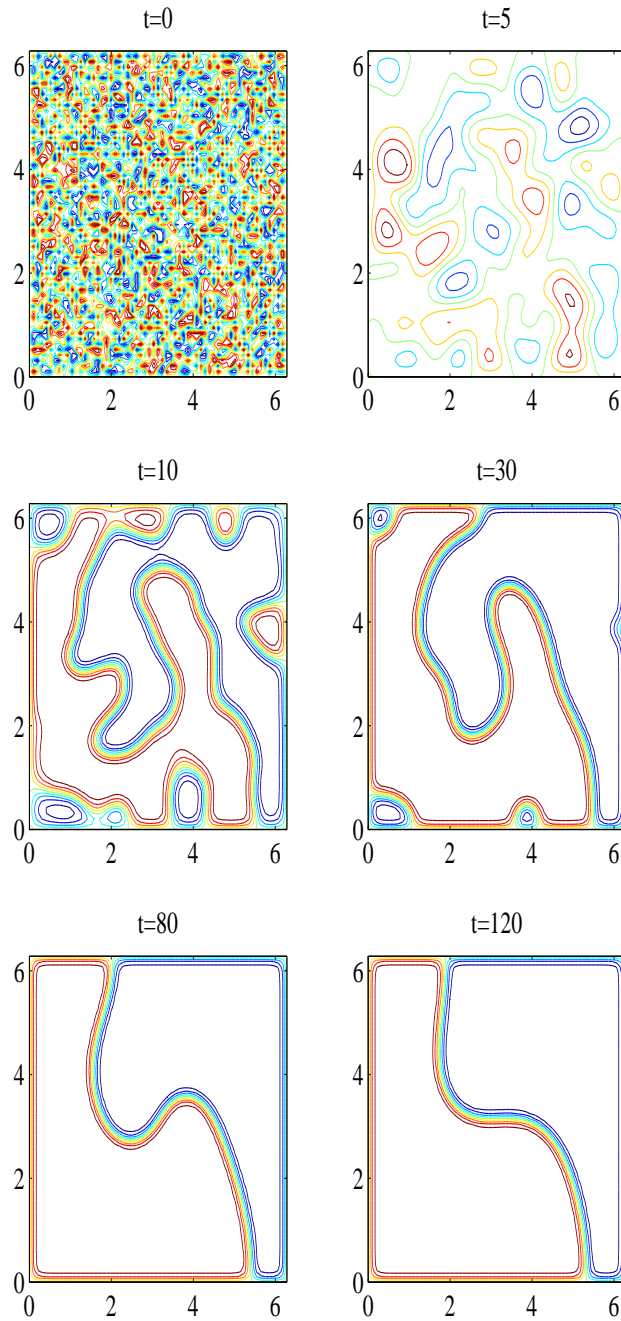


FIGURE 7. Example 4.3: the solution evolution of 2D Allen-Cahn equation with random initial distribution.

REFERENCES

- [1] S. M. Allen and J. W. Cahn, *A microscopic theory for antiphase boundary motion and its application to antiphase domain coarsening*, Acta Metall, **27** (1979), 1085–1095.
- [2] U. M. Ascher, J. Ruuth and R. J. Spiteri, *Implicit-explicit Runge-Kutta method for time dependent partial differential equations*, Special issue on time integration (Amsterdam, 1996), Appl. Numer. Math., **25** (1997), 151–167.
- [3] U. M. Ascher, J. Ruuth and T. R. Wetton, *Implicit-explicit method for time dependent partial differential equations*, SIAM J. Numer. Anal., **32** (1995), 797–823.
- [4] A. L. Bertozzi, N. Ju and H.-W. Lu, *A biharmonic modified forward time stepping method for fourth order nonlinear diffusion equations*, Discrete Contin. Dyn. Syst. A, **29** (2011), 1367–1391.
- [5] A. L. Bertozzi, S. Esedoglu and A. Gillette, *Analysis of a two-scale Cahn-Hilliard model for image inpainting*, Multiscale Model. Simul., **6** (2007), 913–936.
- [6] A. L. Bertozzi, S. Esedoglu and A. Gillette, *Inpainting of binary images using the Cahn-Hilliard equation*, IEEE Trans. Image Proc., **16** (2007), 285–291.
- [7] S. Boscarino, L. Pareschi and G. Russo, *Implicit-explicit Runge-Kutta schemes for hyperbolic systems and kinetic equations in the diffusion limit*, SIAM J. Sci. Comput., **35** (2013), A22–A51.
- [8] F. Chen and J. Shen, *Efficient energy stable schemes with spectral discretization in space for anisotropic Cahn-Hilliard systems*, Commun. Comput. Phys., **13** (2013), 1189–1208.
- [9] C. Collins, J. Shen and S. M. Wise, *An efficient, energy stable scheme for the Cahn-Hilliard-Brinkman system*, Commun. Comput. Phys., **13** (2013), 929–957.
- [10] Charles M. Elliott and Bjorn Stinner, *Computation of two-phase biomembranes with phase dependent material parameters using surface finite elements*, Commun. Comput. Phys., **13** (2013), 325–360.
- [11] D. J. Eyre, *An unconditionally stable one-step scheme for gradient systems*, unpublished article, 1998. <http://www.math.utah.edu/eyre/research/methods/stable.ps>
- [12] X. Feng, T. Tang and J. Yang, *Stabilized Crank-Nicolson/Adams-Bashforth schemes for phase field models*, East Asian J. Appl. Math., **3** (2013), 59–80.
- [13] L. Golubovic, A. Levandovsky and D. Moldovan, *Interface dynamics and far-from-equilibrium phase transitions in multilayer epitaxial growth and erosion on crystal surfaces: Continuum theory insights*, East Asian J. Appl. Math., **1** (2011), 297–371.
- [14] F. de la Hoz and F. Vadillo, *A Sylvester-based IMEX method via differentiation matrices for solving nonlinear parabolic equations*, Commun. Comput. Phys., **14** (2013), 1001–1026.
- [15] Y. He, Y. Liu and T. Tang, *On large time-stepping methods for the Cahn-Hilliard equation*, Appl. Numer. Math., **57** (2007), 616–628.
- [16] Samet Y. Kadioglu and Dana A. Knoll, *A Jacobian-free Newton Krylov implicit-explicit time integration method for incompressible flow problems*, Commun. Comput. Phys., **13** (2013), 1408–1431.
- [17] A. Kassam and L. N. Trefethen, *Fourth-order time-stepping for stiff PDEs*, SIAM J. Sci. Comput., **26** (2005), 1214–1233.
- [18] Junseok Kim, *Phase-field models for multi-component fluid flows*, Commun. Comput. Phys., **12** (2012), 613–661.
- [19] M. Li, T. Tang and B. Fornberg, *A compact fourth-order finite difference scheme for the steady incompressible Navier-Stokes equations*, Int. J. Numer. Methods Fluids, **20**(1995), 1137–1151.
- [20] M. Li and T. Tang, *A compact fourth-order finite difference scheme for unsteady viscous incompressible flows*, J. Sci. Comp., **16**(2001), 29–45.
- [21] B. Li and J.-G. Liu, *Thin film epitaxy with or without slope selection*, European J. Appl. Math., **14** (2003), 713–743.
- [22] Z. Qiao, Z. Sun and Z. Zhang, *The stability and convergence of two linearized finite difference schemes for the nonlinear epitaxial growth model*, Numer. Meth. Part Differ. Equ., **28** (2012), 1893–1915.
- [23] Z. Qiao, Z. Zhang and T. Tang, *An adaptive time-stepping strategy for the molecular beam epitaxy models*, SIAM J. Sci. Comput., **33** (2011), 1395–1414.
- [24] J. Shen, T. Tang and L. Wang, “Spectral Methods: Algorithms, Analysis and Applications,” **41** Springer, Heidelberg, 2011, xvi+470 pp.

- [25] J. Shen and X. Yang, *Numerical approximations of Allen-Cahn and Cahn-Hilliard equations*, Discrete Contin. Dyn. Syst. A, **28** (2010), 1669–1691.
- [26] C. Xu and T. Tang, *Stability analysis of large time-stepping methods for epitaxial growth models*, SIAM J. Numer. Anal., **44** (2006), 1759–1779.
- [27] X. Yang, *Error analysis of stabilized semi-implicit method of Allen-Cahn equation*, Discrete Contin. Dyn. Syst. Ser. B, **11** (2009), 1057–1070.
- [28] J. Zhang and Q. Du, *Numerical studies of discrete approximations to the Allen-Cahn equation in the sharp interface limit*, SIAM J. Sci. Comput., **31** (2009), 3042–3063.
- [29] Z. Zhang and Z. Qiao, *An adaptive time-stepping strategy for the Cahn-Hilliard equation*, Commun. Comput. Phys., **11** (2012), 1261–1278.

Received November 2012; revised June 2013.

E-mail address: fxlmath@gmail.com

E-mail address: songhuailing@gmail.com

E-mail address: ttang@hkbu.edu.hk

E-mail address: jiangy@hkbu.edu.hk